Supplementary Information

Quantifying antiviral activity optimizes drug combinations against hepatitis C virus infection

Yoshiki Koizumi[1], Hirofumi Ohashi[2,3], Syo Nakajima[2,3], Yasuhito Tanaka[4], Takaji Wakita[2], Alan S. Perelson[5], Shingo Iwami[6,7,8,†,*], & Koichi Watashi[2,3,8,†,*]

[1]School of Medicine, College of Medical, Pharmaceutical and Health Sciences, Kanazawa University, Ishikawa 920-8640, Japan. [2]Department of Virology II, National Institute of Infectious Diseases, Tokyo 162-8640, Japan. [3]Department of Applied Biological Sciences, Faculty of Science and Technology, Tokyo University of Sciences, Chiba 278-8510, Japan. [4]Department of Virology and Liver Unit, Nagoya City University Graduate School of Medicinal Sciences, Nagoya 467-8601, Japan. [5]Theoretical Biology and Biophysics Group, Los Alamos National Laboratory, Los Alamos, NM 87501, USA. [6]Department of Biology, Faculty of Sciences, Kyushu University, Fukuoka 812-8581, Japan. [7]PRESTO, JST, Saitama 332-0012, Japan. [8]CREST, JST, Saitama 332-0012, Japan.

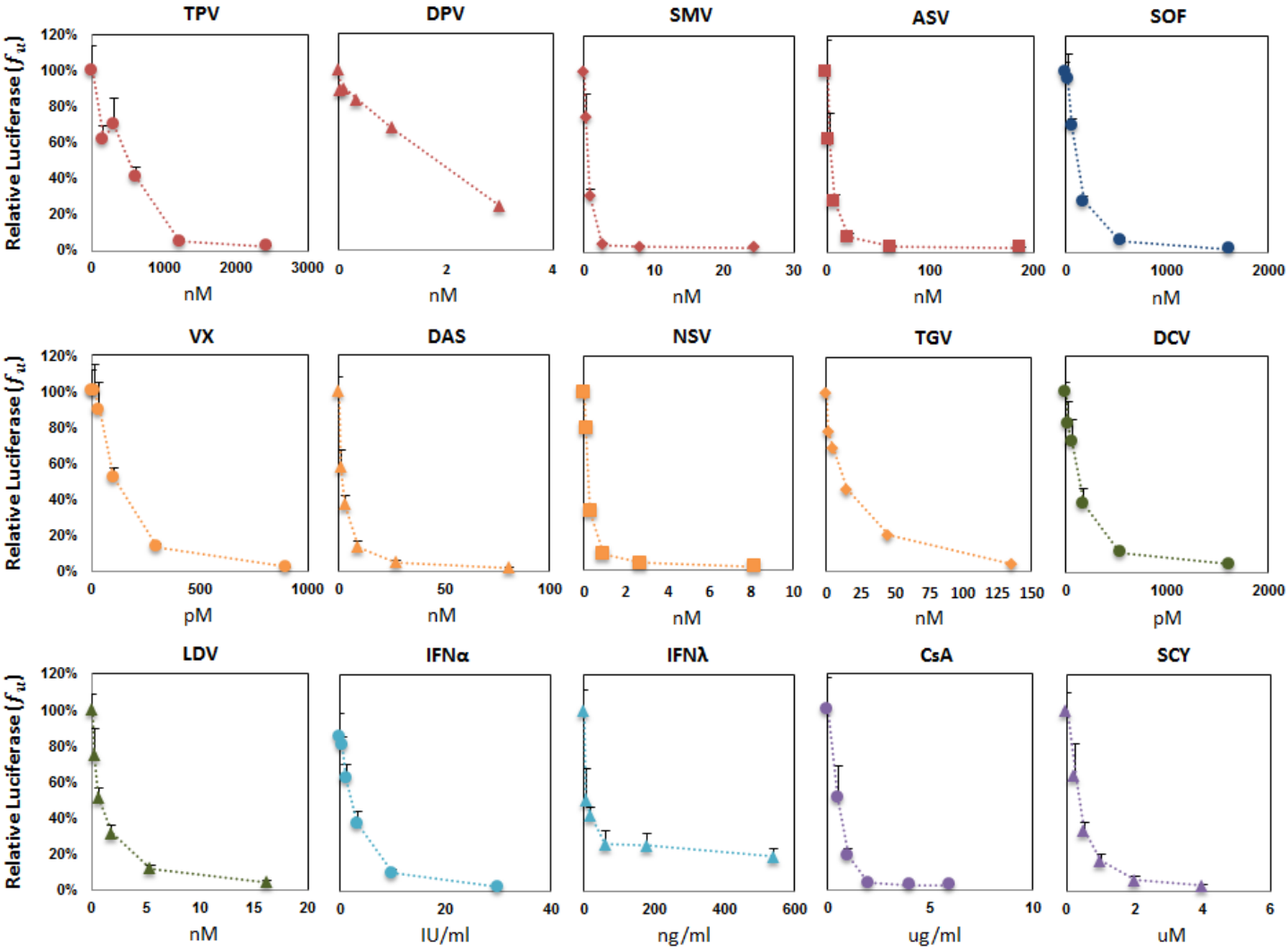

Figure S1. Dose-response curves of PIs (TPV, DPV, SMV, ASV: red), NI (SOF: blue), NNIs (VX, DAS, NSV, TGV: orange), NS5AIs (DCV, LDV: green), IFNs (IFN-α, IFN-λ: cyan), and CIs (CsA, SCY: purple), obtained by HCV replicon assay. Each point represents the mean ± standard deviation (s.d.) of three experiments.

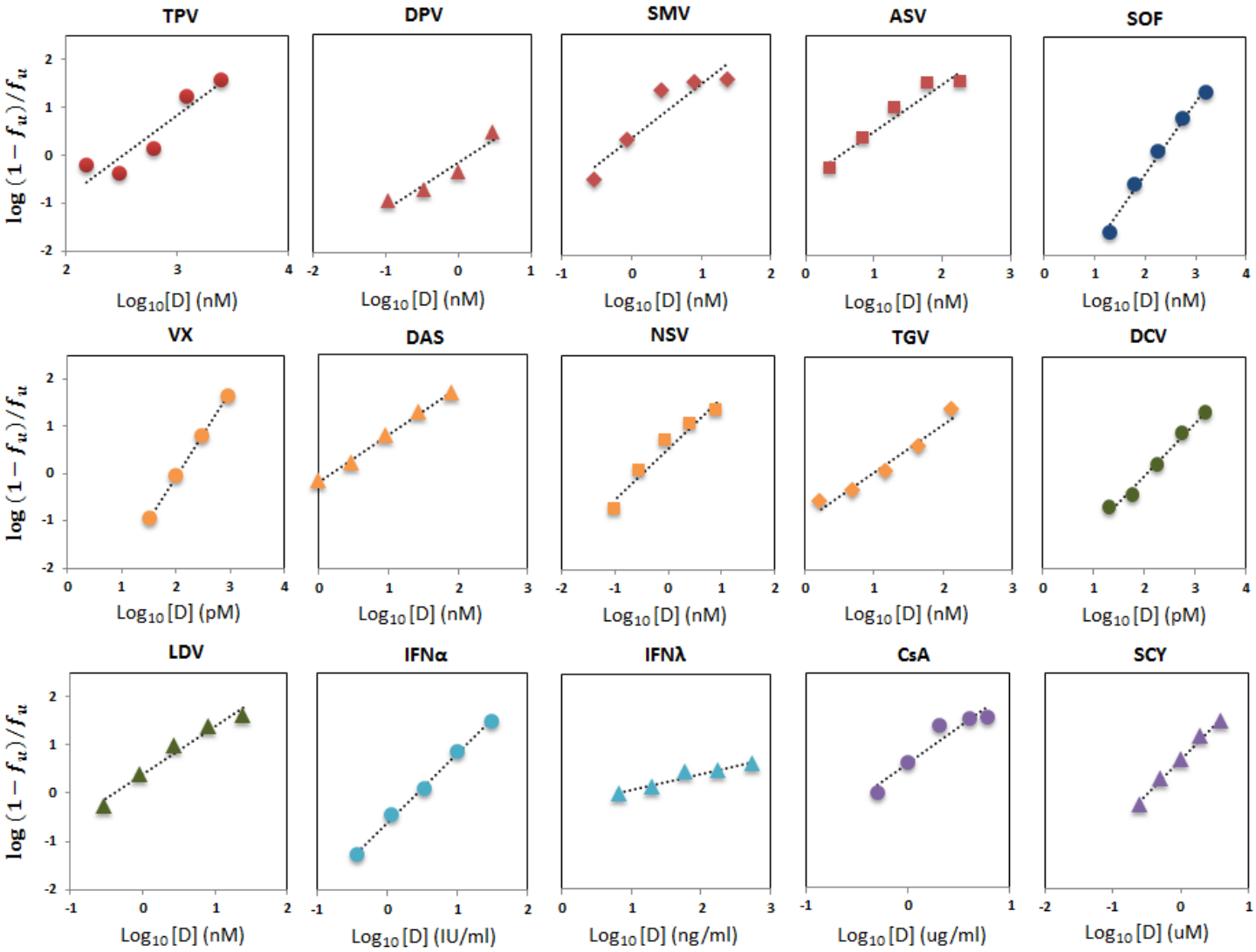

Figure S2. Median effect plots for PIs (TPV, DPV, SMV, ASV: red), NI (SOF: blue), NNIs (VX, DAS, NSV, TGV: orange), NS5AIs (DCV, LDV: green), IFNs (IFN-α, IFN-λ: cyan), and CIs (CsA, SCY: purple), obtained by HCV replicon assay. Each point represents the mean of three experiments. The dashed lines are predicted from $m \log(D/IC_{50})$ in Eq. (1) using the best-fitted parameters.

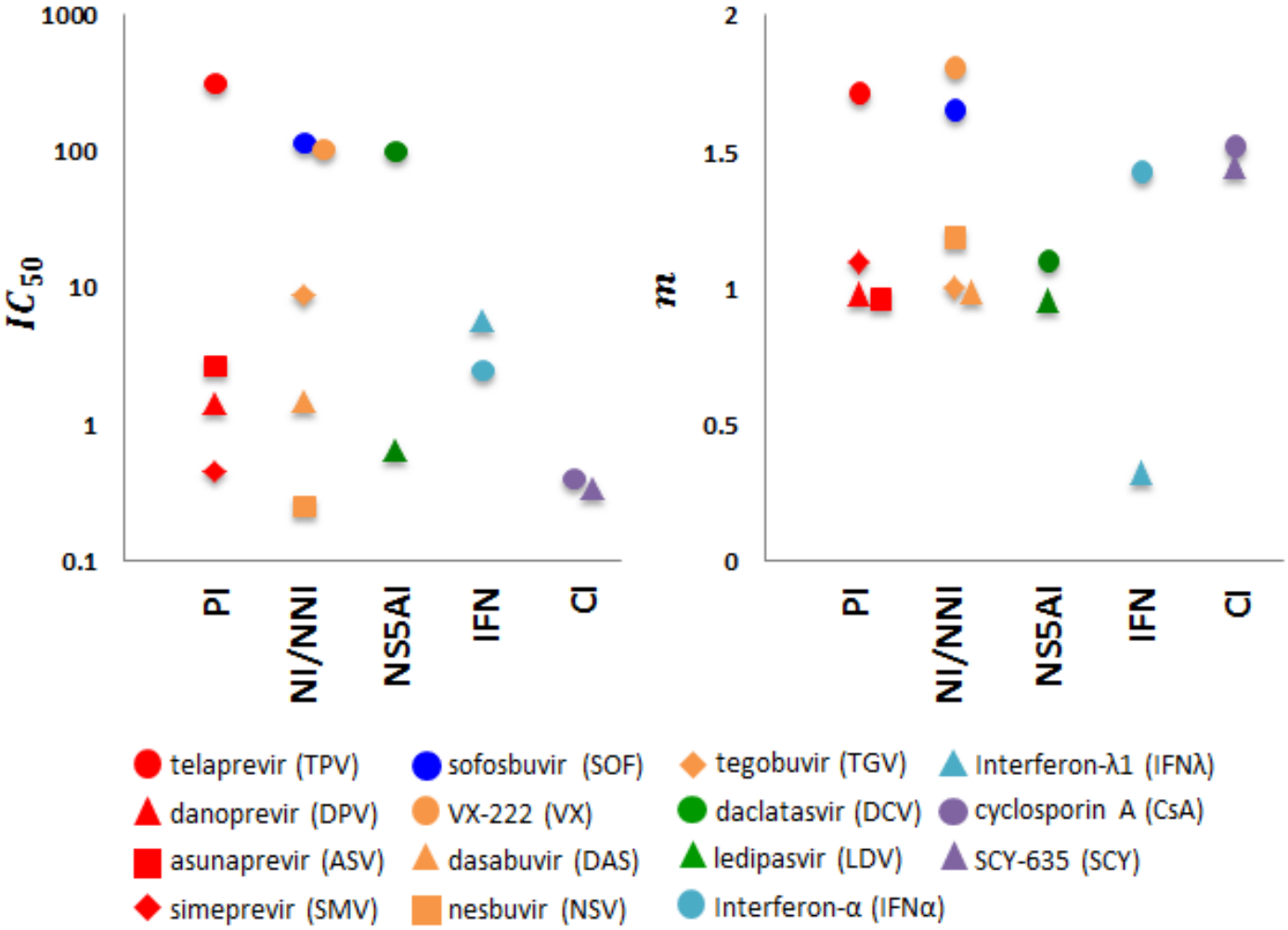

Figure S3. IC_{50} and m value for each drug, estimated by fitting Eq. (2) to the corresponding median effect plot, are grouped into drug classes or subclasses. Unit of IC_{50} is nM; exceptions are VX and DCV (pM), IFN-α (IU/ml), IFN-λ (ng/ml), CsA (μg/ml), and SCY (μM).

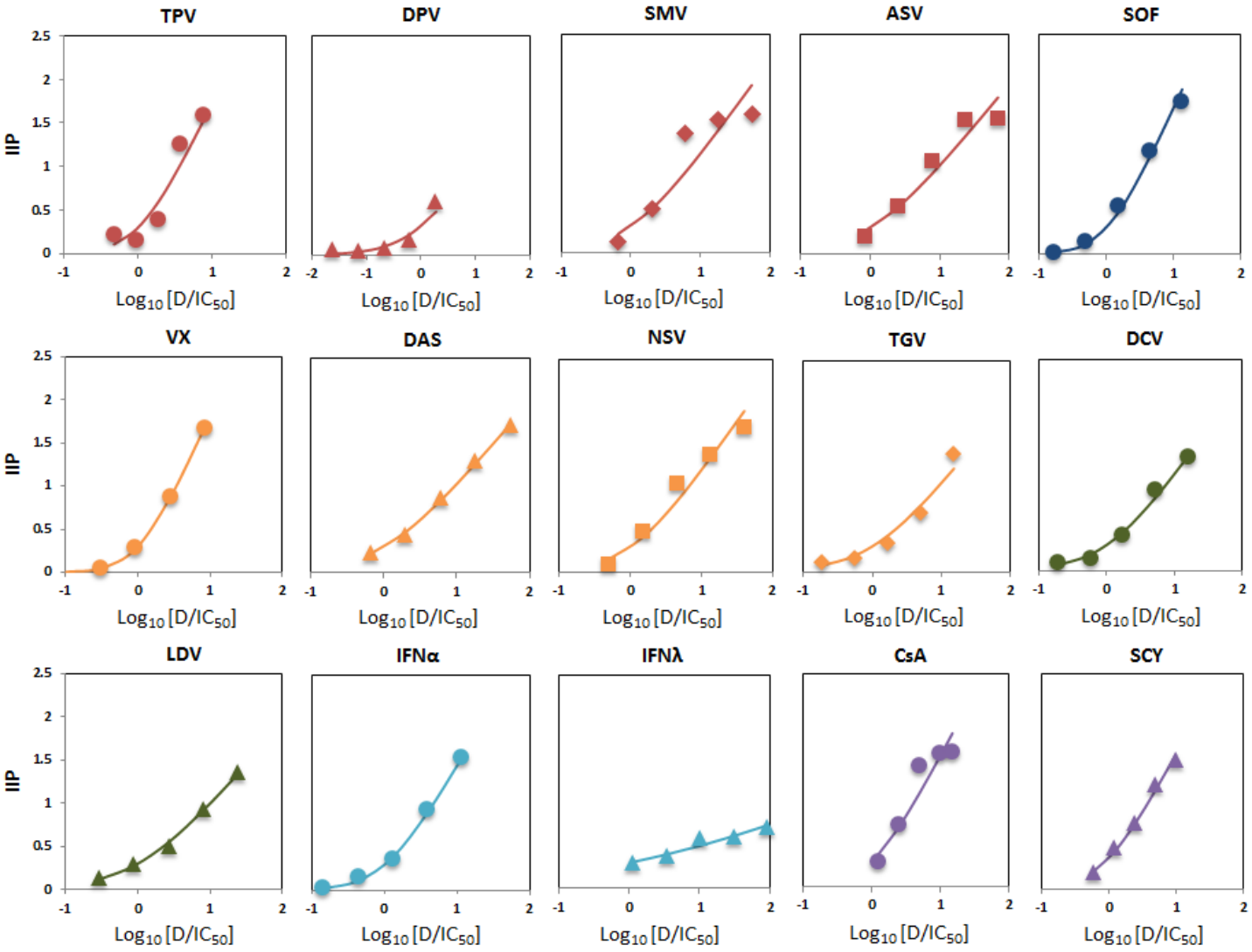

Figure S4. Instantaneous inhibitory potential (IIP) of PIs (TPV, DPV, SMV, ASV: red), NI (SOF: blue), NNIs (VX, DAS, NSV, TGV: orange), NS5AIs (DCV, LDV: green), IFNs (IFN-α, IFN-λ: cyan), and CIs (CsA, SCY: purple), obtained by HCV replicon assay. Each point represents the mean of three experiments. The solid lines are predicted from $\log[1 + (D/IC_{50})^m]$ in Eq. (1) using the parameters estimated from the median effect plots (Fig. S2).

Figure S5. Dose-response curves of the 52 double-combinations of inter-class (sub-class) antiviral drugs selected for the study, obtained by HCV replicon assay. Each point represents the mean $\pm$ s.d. of four experiments. Drugs were concentrated by constant ratios from their initial concentrations $D_{\text{initial}} = 0.25 \times IC_{50}$ to a maximum concentration of $4 \times IC_{50}$.

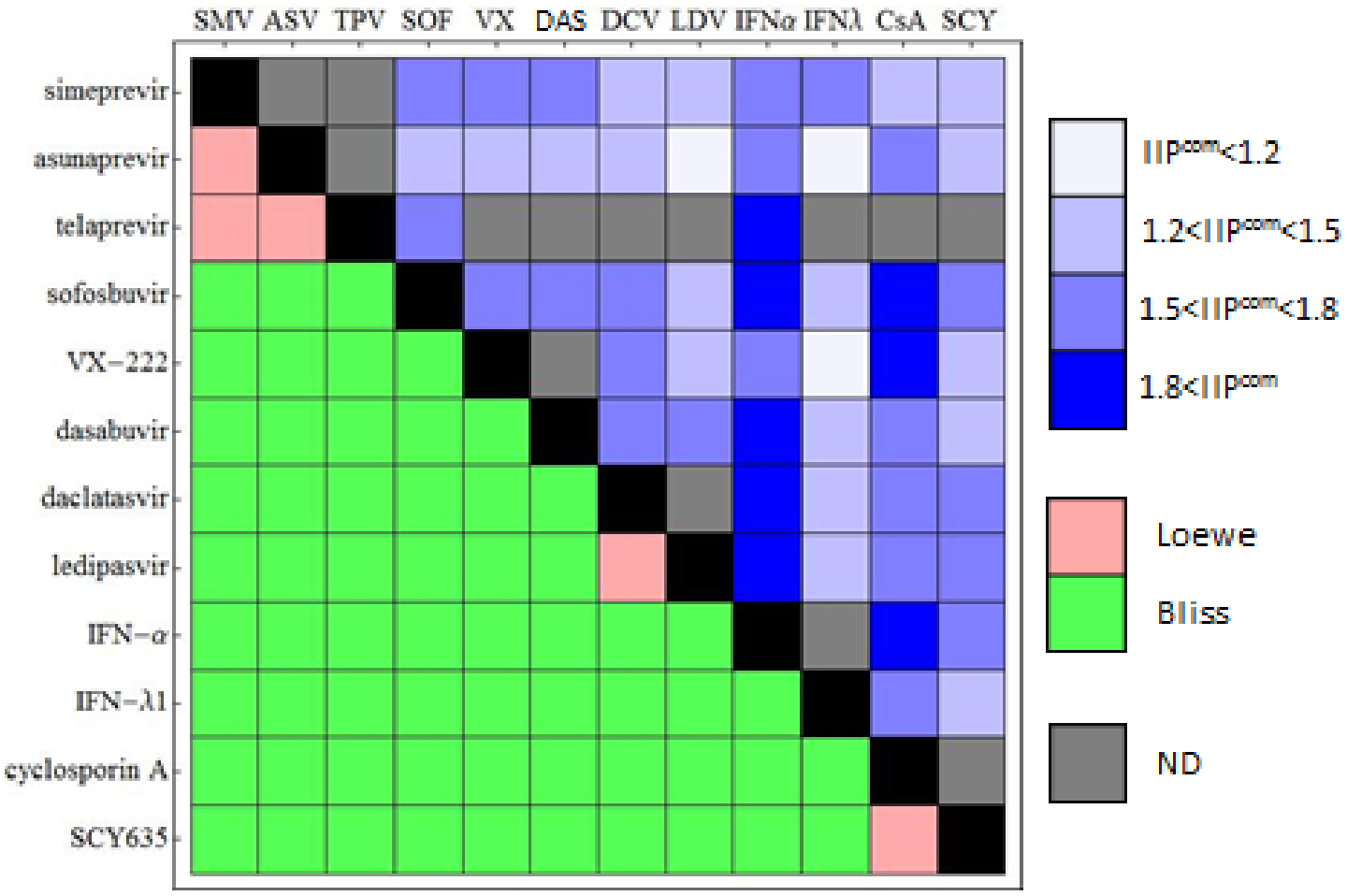

Figure S6. Lower triangular elements show the expected combination effects based on the binding-site criterion. Upper triangular elements show the observed combination effects categorized by IIP^{com} values at the final concentration $4 \times IC_{50}$. ND, not determined.

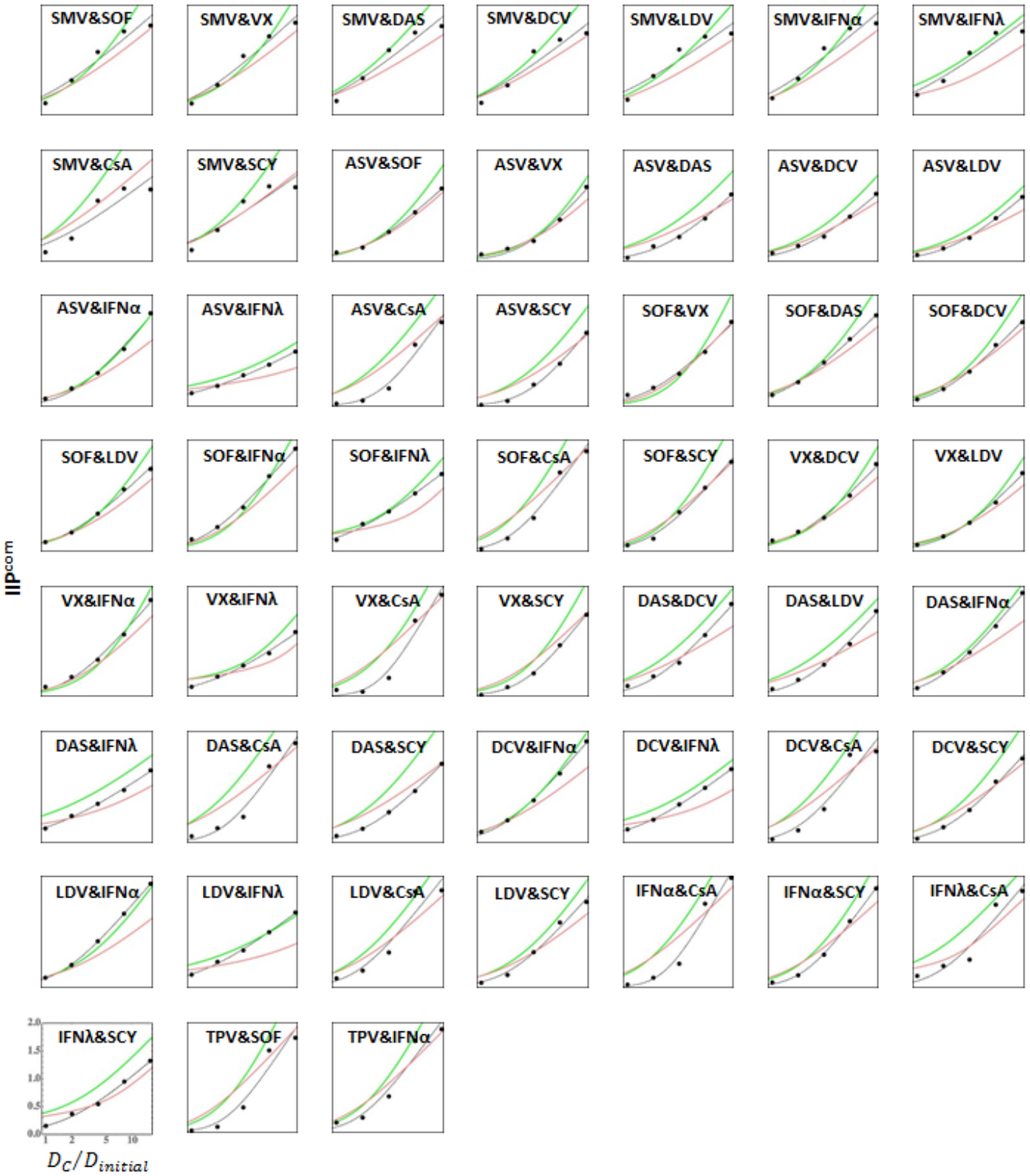

Figure S7. Instantaneous inhibitory potentials of the 52 tested drug combinations (IIP^{com}), calculated as $\log(1/f_u^{com})$ of the experimentally determined f_u^{com} values (black dots). The pink and green lines are the IIP^{com}s predicted by Loewe additivity and Bliss independence, respectively. The black lines are the theoretical predictions of $\log\{1 + [(D_c/D_{initial})/IC_{50}^{com}]^{m^{com}}\}$ using the best-fitted parameters.

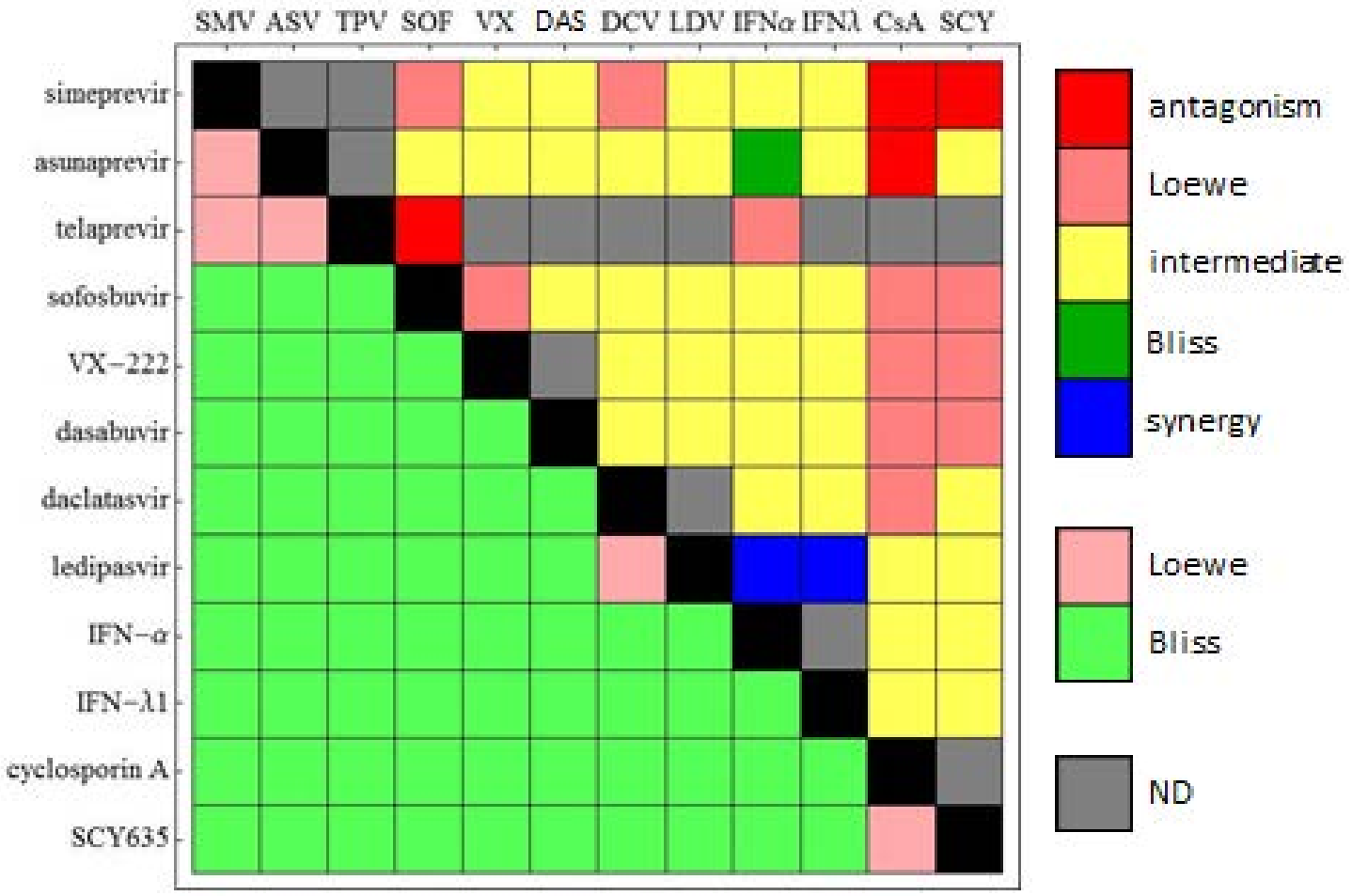

Figure S8. Lower triangular elements show the expected combination effects based on the binding-site criterion. Upper triangular elements show the observed combination effects categorized by DI values at $4 \times IC_{50}$: antagonism, DI < −0.1; Loewe, −0.1 < DI < 0.1; intermediate, 0.1 < DI < 0.9; Bliss, 0.9 < DI < 1.1; synergy, 1.1 < DI. ND, not done. Among the 52 combinations of inter-class (sub-class) antiviral drugs, 65% showed intermediate activity.

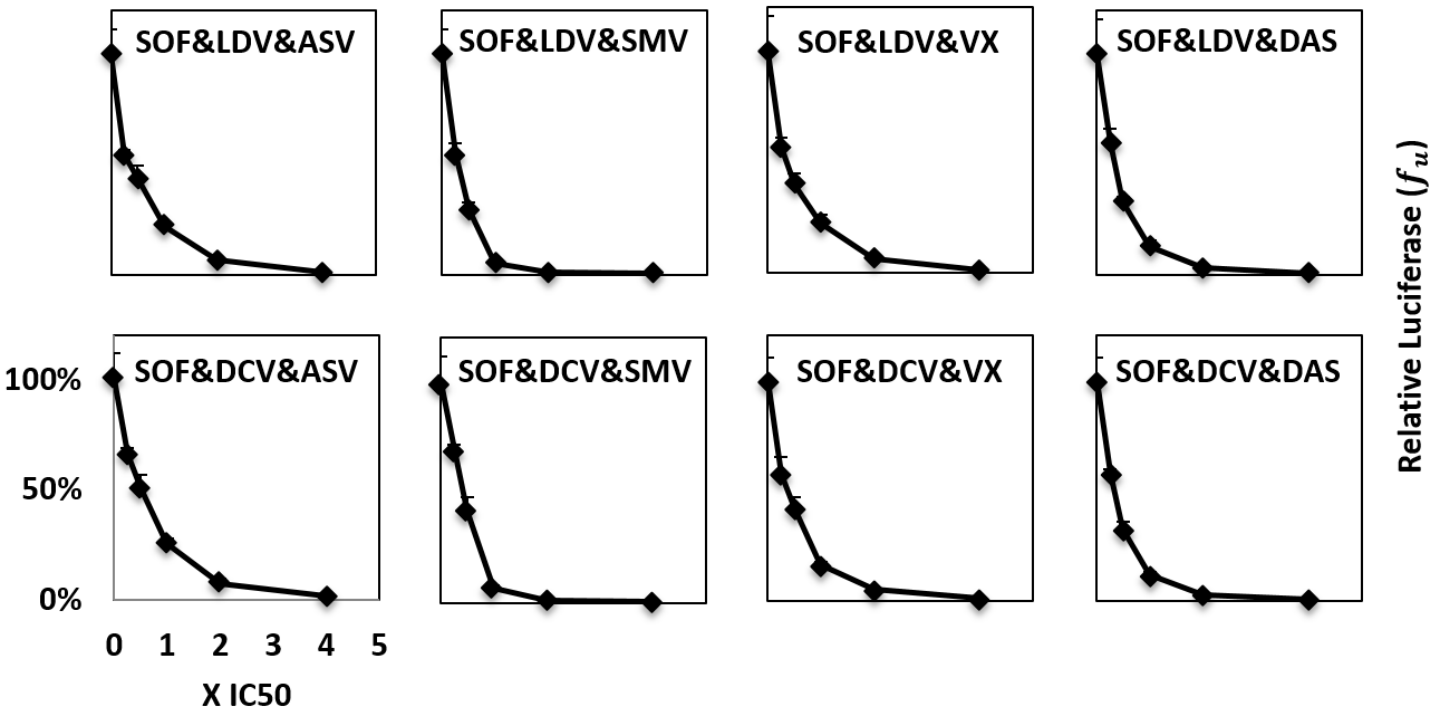

Figure S9. Dose-response curves of the 8 triple-combinations of inter-class (sub-class) antiviral drugs selected for the study, obtained by HCV replicon assay. Each point represents the mean $\pm$ s.d. of five experiments. Drugs were concentrated by constant ratios from their initial concentrations $D_{\text{initial}} = 0.25 \times IC_{50}$ to a maximum concentration of $4 \times IC_{50}$.

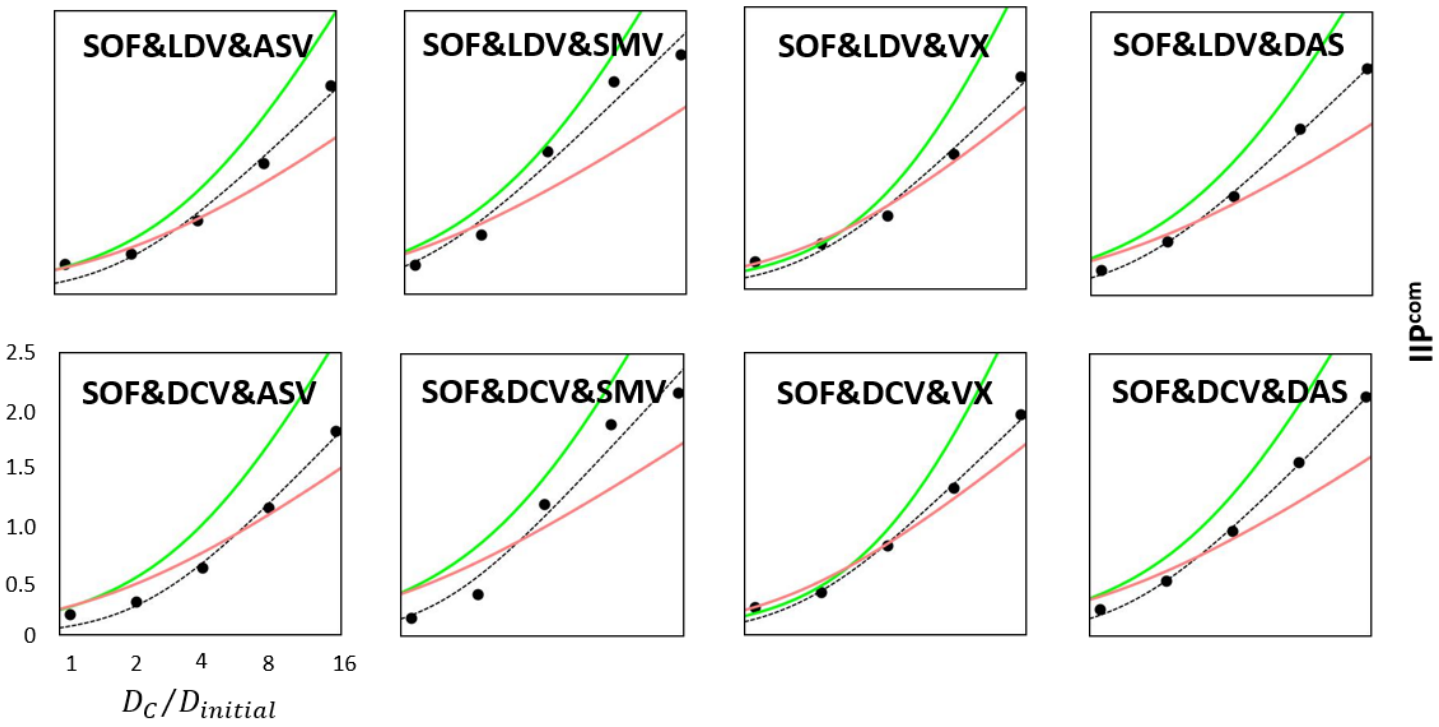

Figure S10. Instantaneous inhibitory potentials of the 8 tested drug combinations (IIP^{com}), calculated as $\log(1/f_u^{\mathrm{com}})$ of the experimentally determined f_u^{com} values (black dots). The pink and green lines are the IIP^{com}s predicted by Loewe additivity and Bliss independence, respectively. The black lines are the theoretical predictions of $\log\{1+[(D_c/D_{initial})/IC_{50}^{\mathrm{com}}]^{m^{\mathrm{com}}}\}$ using the best-fitted parameters.

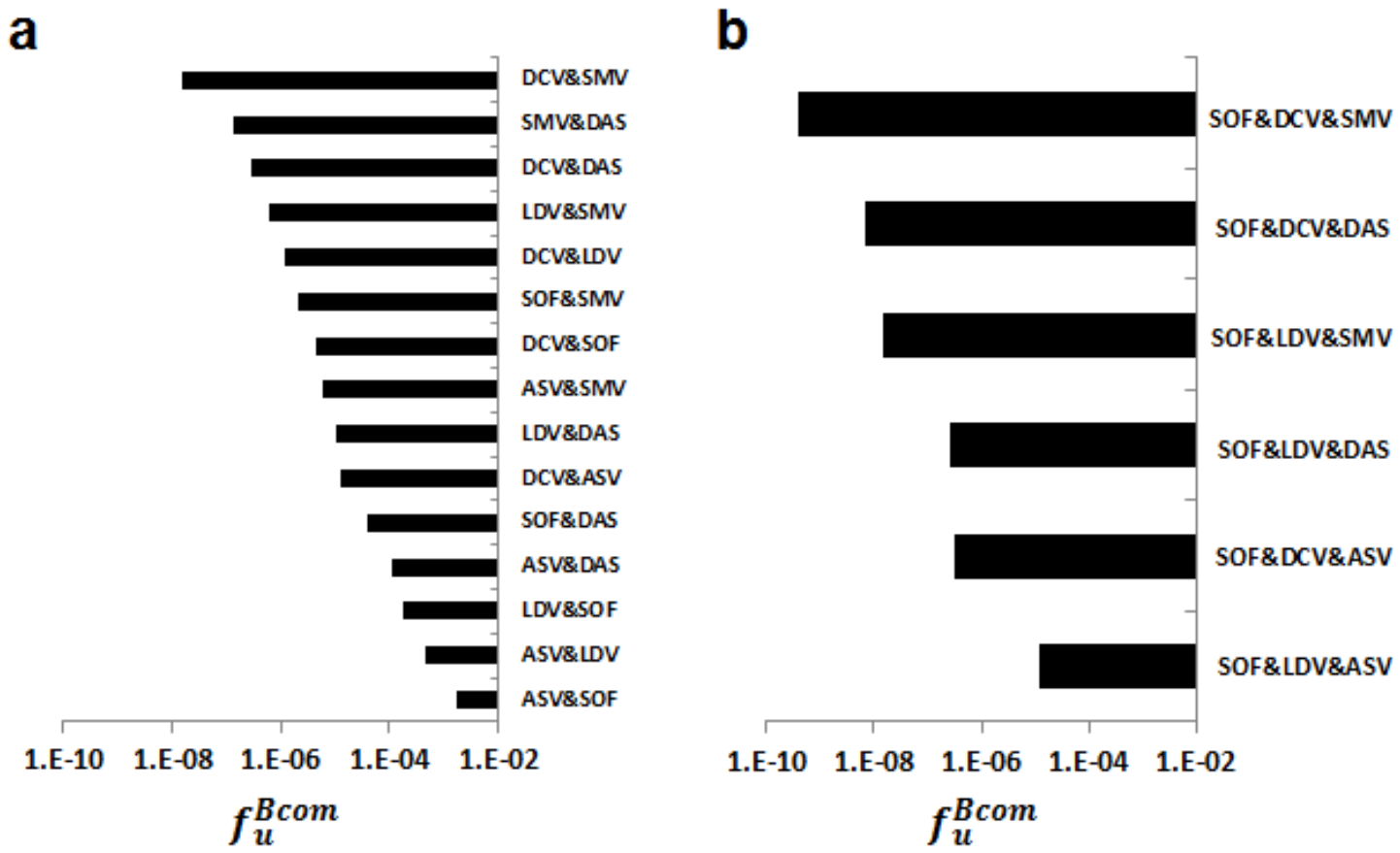

Figure S11. The fraction of unaffected HCV replication events f_u^{Bcom} of each **(a)** double-drug and **(b)** triple-drug combination at clinical concentrations.

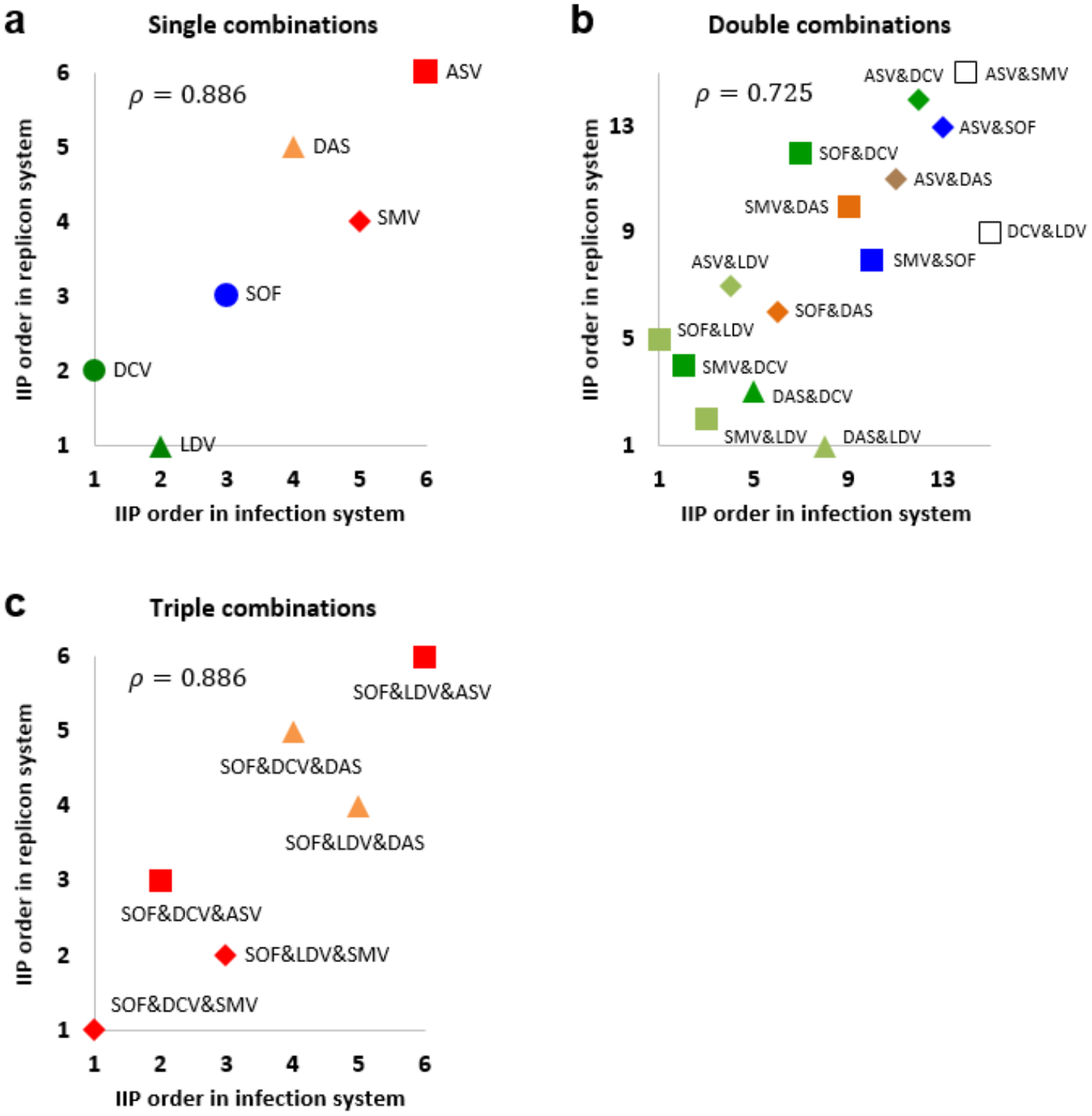

Figure S12. Spearman's rank-order correlation for IIPs (IIP^{com}s) of anti-HCV drugs in (a) single treatment, and (b) double and (c) triple combinations for the HCV JFH-1 (genotype-2) replicon and the infectious systems.

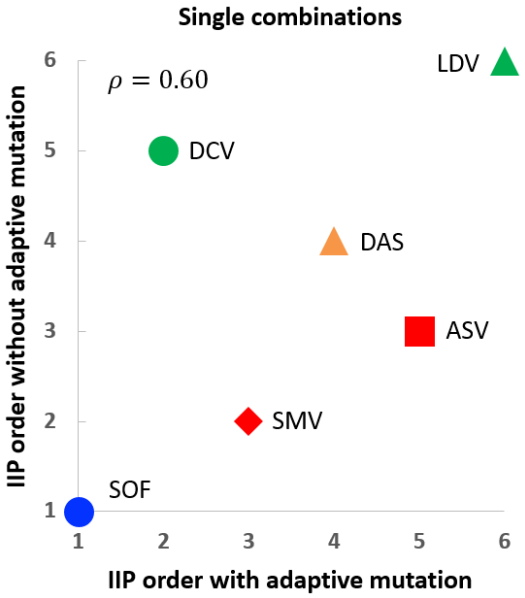

Figure S13. Spearman's rank-order correlation for IIPs of anti-HCV drugs in single treatment for an HCV genotype-1 replicon with and without cell culture-adaptive mutations.

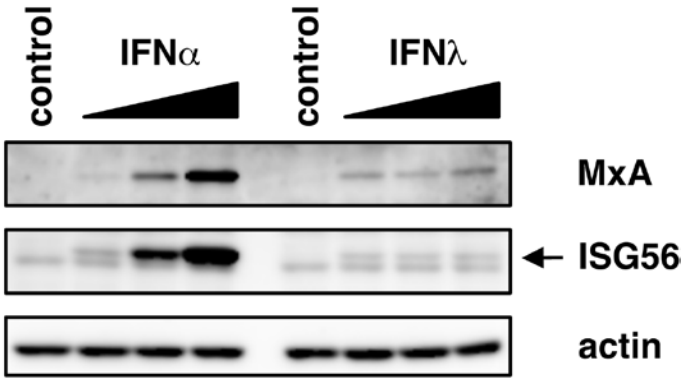

Figure S14. Induction of IFN stimulated genes (ISGs) by IFN-α and IFN-λ. Protein expressions of MxA and ISG56 as representative ISGs and actin as an internal control in LucNeo#2 cells treated with varying concentrations of IFN-α (10, 30, and 90 IU/ml) and IFN-λ (180, 540, and 1620 ng/ml) or left untreated (control). The arrow shows a band for ISG56.

Table S1 | Estimated characteristic parameters of the tested antiviral drugs

Drug (unit)	Class	IC_{50}	m
TPV (nM)	PI	323.79	1.72
DPV (nM)	PI	1.40	0.98
SMV (nM)	PI	0.45	1.10
ASV (nM)	PI	2.75	0.97
SOF (nM)	NI	120.48	1.66
VX (pM)	NNI	107.58	1.81
DAS (nM)	NNI	1.50	0.99
NSV (nM)	NNI	0.25	1.19
TGV (nM)	NNI	8.92	1.01
DCV (pM)	NS5AI	103.84	1.11
LDV (nM)	NS5AI	0.67	0.96
IFNα (IU/ml)	IFN	2.56	1.43
IFNλ (ng/ml)	IFN	5.80	0.33
CsA (μg/ml)	CI	0.40	1.53
SCY (μM)	CI	0.34	1.45

Table S2 | Estimated characteristic parameters of the antiviral drug combinations

Drug combinations (Drug A and B)	IIP of final concentration	DI of final concentration	IC_{50}^{com} of combination	m^{com} of combination
SMV & IFNα	1.671	0.192	0.689	1.337
SMV & DAS	1.620	0.218	0.712	1.306
SMV & SOF	1.631	0.074	0.808	1.377
TPV & IFNα	1.883	0.071	1.838	2.144
SMV & VX	1.678	0.253	0.960	1.453
SMV & IFNλ	1.526	0.493	0.614	1.181
LDV & CsA	1.748	0.170	1.714	1.991
SMV & LDV	1.481	0.199	0.577	1.137
LDV & IFNα	1.863	1.150	1.527	1.819
SOF & IFNα	1.841	0.529	1.463	1.766
DAS & IFNα	1.879	0.761	1.582	1.838
IFNα & CsA	1.971	0.225	2.688	2.671
SMV & DCV	1.490	0.078	0.801	1.257
DCV & IFNα	1.819	0.770	1.607	1.789
SOF & CsA	1.800	-0.048	2.196	2.183
IFNλ & CsA	1.737	0.308	1.807	1.906
DCV & CsA	1.641	-0.071	1.990	2.016
TPV & SOF	1.726	-0.191	2.568	2.365
DAS & CsA	1.785	0.099	2.380	2.228
VX & CsA	1.847	0.071	3.065	2.710
IFNα & SCY	1.779	0.373	2.346	2.135
VX & IFNα	1.754	0.632	1.884	1.830
SOF & DAS	1.633	0.326	1.375	1.529
SMV & SCY	1.334	-0.290	0.759	1.142
DAS & DCV	1.679	0.631	1.872	1.750
SOF & SCY	1.608	0.039	1.995	1.799
ASV & IFNα	1.673	1.096	2.117	1.835
LDV & SCY	1.540	0.379	2.064	1.785
SMV & CsA	1.292	-0.502	0.938	1.204
SOF & DCV	1.510	0.189	1.895	1.637
DCV & SCY	1.515	0.148	2.132	1.751
SOF & LDV	1.480	0.362	1.668	1.520
VX & DCV	1.565	0.502	1.873	1.612
ASV & CsA	1.513	-0.181	3.186	2.250
DAS & LDV	1.551	0.674	2.175	1.722
SOF & VX	1.515	0.036	1.886	1.567
VX & SCY	1.483	-0.052	3.057	2.054
SOF & IFNλ	1.388	0.527	1.237	1.236
DAS & SCY	1.419	-0.010	2.278	1.640
VX & LDV	1.405	0.499	2.358	1.632
LDV & IFNλ	1.349	1.126	1.264	1.196
DCV & IFNλ	1.323	0.724	1.307	1.196
IFNλ & SCY	1.327	0.281	1.813	1.375
ASV & SCY	1.322	0.106	3.502	1.967
ASV & SOF	1.309	0.184	2.177	1.474
ASV & VX	1.338	0.612	3.099	1.783
DAS & IFNλ	1.299	0.534	1.125	1.092
ASV & DAS	1.207	0.206	2.604	1.475
ASV & DCV	1.216	0.350	2.361	1.405
ASV & LDV	1.161	0.598	2.610	1.427
VX & IFNλ	1.169	0.461	1.756	1.156
ASV & IFNλ	0.983	0.660	1.396	0.884

Table S3 | Estimated characteristic parameters of the antiviral drug combinations

Drug combinations (Drug A, B and C)	IIP of final concentration	DI of final concentration	IC_{50}^{com} of combination	m^{com} of combination
SOF&LDV&ASV	1.843	0.457	1.848	1.879
SOF&LDV&SMV	2.117	0.336	1.025	1.899
SOF&LDV&VX	1.883	0.261	1.794	1.896
SOF&LDV&DAS	2.003	0.382	1.388	1.881
SOF&DCV&ASV	1.809	0.310	2.189	2.031
SOF&DCV&SMV	2.157	0.298	1.328	2.144
SOF&DCV&VX	1.952	0.233	1.632	1.919
SOF&DCV&DAS	2.123	0.385	1.360	1.970

Table S4 | Clinical concentrations of drugs (C_{trough})

Drug	Concentration (nM)	References
ASV	40	(1)
SMV	2200	(1)
SOF	1100	(1)
DAS	1033	(2)*
DCV	250	(1)
LDV	120	(1)

* The unit of clinical concentration in (2) 0.51 ug/ml, is converted to nM.

Supplementary Note 1: Profiling intrinsic antiviral activity of single HCV drugs

The typical dose-response curve (**Supplementary Fig. S1**) of a single antiviral drug can be analyzed by the following median effect model (3-8):

$$\log\left(\frac{1-f_u}{f_u}\right) = m\log\left(\frac{D}{IC_{50}}\right). \qquad (S1)$$

Here, $1-f_u$ and f_u are the fractions of infection events affected and unaffected by the drug, respectively, D is the drug concentration, IC_{50} is the drug concentration that inhibits 50% inhibition of the activity, and m is the slope parameter reflecting the steepness of the dose-response curve (3-8). The log–log dose-response curves (**Fig. 2a**) were converted into median effect plots by transforming $\log f_u$ into $\log(1-f_u)/f_u$ (**Supplementary Fig. S2**). The IC_{50} and slope parameter m were estimated by linear regression of the data plotted in the median effect plot as the intercept with 0 and the slope, respectively (**Supplementary Fig. S2**, **S3** and **Table S1**).

The IC_{50} is widely used to measure drug potency, but the slope parameter m, which can vary with the drug class (6), also substantially affects the antiviral activity (3-8). In this assay, we used interferon-α (IFN-α) instead of peg-IFN-α as an IFN-based drug. As the antiviral activity of these two drugs is equivalent in cell cultures (9), the intrinsic antiviral effect of peg-IFN-α can be interpreted from the data for IFN-α in this study. Interestingly, we found that past and present first-line anti-HCV drugs (10-12), namely, IFN-α, TPV and SOF, had relatively high m values (around 1.5 or higher; **Supplementary Fig. S3**), confirming the high anti-HCV potential of these drugs. Cyclophilin inhibitors (CIs) such as cyclosporin A (CsA) and SCY-635 (SCY) exhibited similarly high m values. This implies that HTAs such as IFN-α and CIs achieve a high antiviral effect at concentrations only slightly above the IC_{50}. Thus, the antiviral activity at drug concentration D is determined not only by the IC_{50} but also by m, which is unique to each drug (3-8).

The IIP of the 15 tested antiviral drugs was calculated from the experimentally measured f_u by $\mathrm{IIP} = \log(1/f_u)$. As shown in **Fig. 2b**, the IIP of the 15 drugs widely varied. The log reductions in HCV replication in the replicon system were well predicted by the equation $\mathrm{IIP} = \log[1+(D/IC_{50})^m]$ (**Supplementary Fig. S4**), using the parameters estimated from the median effect plot in **Supplementary Fig. S3**. Classifying the 15 drugs used into groups: protease inhibitors (PIs), nucleoside and non-nucleoside polymerase inhibitors (NI and NNIs, respectively), NS5A inhibitors (NS5AI), IFN and cyclophilin inhibitors (CI), we found that drugs in the same class all had similar IIPs when normalized by the drug's IC_{50} (**Fig. 2b**).

The IIP values depended on the subclass of antiviral agent. TPV showing high IIP is a linear ketoamide-type PI, while all the other PIs that had relatively low IIP (DPV, ASV, and SMV) are

macrocyclic PIs (13). Among polymerase inhibitors, SOF, a NI, and VX, an allosteric polymerase inhibitor that binds to site 2 of the thumb domain of the polymerase, showed high IIP. In contrast, all the palm domain-targeting NNIs (DAS, NSV, and TGV) had low IIP values (14). Agents that target NS5A (DCV and LDV) had low IIPs, but those inhibiting cyclophilins (CsA and SCY) had consistently high IIPs. Thus, IIP values tended to depend on the subclass of antiviral agent. While SOF is known to have a high barrier to drug resistance (15), our data indicate that this drug also has a high antiviral activity, based on IIP analysis, which is likely to explain another aspect of the superiority of SOF. In this study, IIP values for IFN-λ were irregularly low; it is likely due to the low induction level of IFN stimulated genes (ISGs) by IFN-λ compared with by IFN-α in our system (**Supplementary Fig. S14**). The molecular basis for determining IIP value remains to be understood, but the agents that have multiple modes of action for antiviral activity, incluDFding IFN-α and CIs (IFN-α induces numerous antiviral factors; CIs inhibit multiple cyclophilins involved in HCV replication (16, 17)), tended to show high IIP values.

Supplementary Note 2: Profiling intrinsic antiviral activity of double-combination HCV drugs

We investigated the antiviral activity of multidrug combinations (i.e., $\mathrm{IIP}^{\mathrm{com}}$). In clinical settings, ribavirin (RBV) augments the antiviral efficacy of IFN-based and DAA-based treatments (11). However, because clinically relevant doses of RBV lack sufficient anti-HCV activity in cell culture systems (18, 19), the antiviral efficacy of RBV was not evaluated. Using the replicon system, the inhibitory activity against HCV replication was evaluated for 52 double-combinations of antiviral drugs (**Supplementary Fig. S5**). In this experiment, drugs were combined so that their initial concentrations were $D_{\mathrm{initial}} = 0.25 \times IC_{50}$ and then the drug concentrations were both increased up to a maximum of 16-fold. Their $\mathrm{IIP}^{\mathrm{com}}$ values were computed from Eq. (1): $\mathrm{IIP}^{\mathrm{com}} = \log(1/f_u^{\mathrm{com}})$, where f_u^{com} are the experimental measurement of a drug combination (**Fig. 3a**). We confirmed that the largest concentration ($4 \times IC_{50}$) of each combination sufficiently suppressed HCV replication without significant cytotoxicity. The combination effects at the largest concentration were categorized by their $\mathrm{IIP}^{\mathrm{com}}$ values, visually presented as the upper triangular elements (blue areas) in **Supplementary Fig. S6** (**Table S2**). In **Supplementary Fig. S7** (and **Fig. S10**), we predicted the $\mathrm{IIP}^{\mathrm{com}}$ of each combination from the measured effects. To produce the black solid lines in **Supplementary Fig. S7** (and **Fig. S10**), we fitted Eq. (S2) to the corresponding experimental data of 52 two-drug and 8 three-drug combinations, respectively:

$$\mathrm{IIP}^{\mathrm{com}} = \log\left[1 + \left(\frac{\widetilde{D}/D_{initial}}{IC_{50}^{\mathrm{com}}}\right)^{m^{\mathrm{com}}}\right], \qquad (S2)$$

where IC_{50}^{com} is the normalized concentration of the combined drugs that inhibits the HCV replication by 50%, m^{com} is the Hill coefficient, and $\widetilde{D}$ is the concentrations of each drugs. Estimated parameter values are listed in **Table S2** and **S3**.

Supplementary Note 3: Anti-viral activity in multiple-drug combinations assessed by the DI index

Pharmacologists assess the combined effect of drugs by two fundamental indices; the Loewe additivity (20-22) and Bliss independence (21-24). We evaluated the combinations for Loewe additivity (20-22) and Bliss independence (21-24), because the combined effects of drugs have been evaluated using these concepts. The Loewe additivity for two (or three) drug A and B (and C) assumes that each drug affects similar targets or pathways, and is expressed as follows:

$$\frac{D_A^*}{D_A} + \frac{D_B^*}{D_B}\left(+\frac{D_C^*}{D_C}\right) = 1, \qquad (S3)$$

where D_A^* and D_B^* (and D_C^*) are the concentrations of the drugs when combined, and D_A and D_B (and D_C) are the concentrations of the single drugs required to produce the antiviral activity of the combined drugs. Substituting the dose response curve $1 - f_u^{com} = D_A^{m_A}/\left(D_A^{m_A} + IC_{50_A}^{m_A}\right)$ or $D_B^{m_B}/\left(D_B^{m_B} + IC_{50_B}^{m_B}\right)$ (or $D_C^{m_C}/\left(D_C^{m_C} + IC_{50_C}^{m_C}\right)$) into D_A and D_B (and D_C) in Eq. (S3), the additive effects of the drug combination are determined as follows:

$$\frac{D_A^*}{IC_{50_A}\left(\frac{1-f_u^{com}}{f_u^{com}}\right)^{\frac{1}{m_A}}} + \frac{D_B^*}{IC_{50_B}\left(\frac{1-f_u^{com}}{f_u^{com}}\right)^{\frac{1}{m_B}}}\left(+\frac{D_C^*}{IC_{50_C}\left(\frac{1-f_u^{com}}{f_u^{com}}\right)^{\frac{1}{m_C}}}\right) = 1. \qquad (S4)$$

We numerically solved Eq. (S4) for f_u^{com}, and thereby predicted the additive effects of the drug combinations (see **Supplementary Fig. S7** and **S10**).

Bliss independence assumes that each drug acts on different targets, and is defined as:

$$f_u^{com} = f_u^A \times f_u^B (\times f_u^C), \qquad (S5)$$

where f_u^{com}, f_u^A and f_u^B (and f_u^C) are the fractions of infection events unaffected by the combined drugs A and B (and C), single drug A and single drug B (and drug C), respectively. Using Eq. (S5), we determined the anti-viral effects of combined drugs A and B (and C), $1 - f_u^{com}$, from the anti-viral effects of the single drugs (see **Supplementary Fig. S7** and **S10**).

To characterize the independence of each drug in experimental data, Jilek et al. (3) proposed a new index called the degree of independence (DI):

$$DI = \frac{F_E - F_L}{F_B - F_L}, \qquad (S6)$$

where F_E, F_B and F_L denote the logarithmic drug effects $(\log[(1 - f_u^{com})/f_u^{com}])$ of experimental data, Bliss independence and Loewe additivity, respectively. Note that this index incorporates both Bliss independence and Loewe additivity, and categorizes the experimental data of combination

effects. From the DI values calculated by Eq. (S6), we assessed the anti-HCV effects of drug combinations (**Supplementary Fig. S8**, **Table S2** and **S3**). Consistent with a previous report for HIV drug combinations (3), most of the two-drug combinations ($\sim 65\%$) exhibited neither Loewe additivity nor Bliss independence but rather had intermediate activity as judged by the Jilek *et al*. (3) degree of independence (DI); see **Supplementary Fig. S8** and **Table S2**.

Supplementary Note 4: Emergence probability of HCV having nucleotides mutants

There are at least two possible mechanisms underlying the emergence of drug resistance in DAA-combination treatments: (I) HCV variants that are resistant to a drug already exist in the HCV quasispecies before treatment and are selected to become the major population under the treatment pressure, (II) mutations that confer drug resistance are introduced by the error-prone polymerase during HCV replication and viruses carrying these mutations expand to be the major population. Each HCV RNA of 9600 nucleotides is synthesized by the NS5B polymerase with an error rate of $\sim 10^{-5}$ per copied nucleotide (25). According to the binomial distribution or its Poisson approximation, Rong *et al.*, estimated the probability of x mutations occurring in the HCV genome after one replication event as follows:

$$P_x = \binom{9600}{x} \times (10^{-5})^x \times (1-10^{-5})^{9600-x}. \quad (S7)$$

Multiplying Eq. (S7) and the total number of HCV virions produced within a patient per day at baseline viral load(26), ~ 10^{12}, we estimated the expected number of newly produced virions per day carrying one-nucleotide substitution, 8.7×10^{10} (i.e., $P_1 \times 10^{12}$). Similarly, the expected number of newly produced virions per day carrying two-nucleotide substitutions is calculated to be 4.2×10^9 (i.e., $P_2 \times 10^{12}$). Because mutation can change a nucleotide to any of three other nucleotides, the number of all possible one-nucleotide and two-nucleotide changed mutants is $\binom{9600}{1} \times 3^1 = 2.9 \times 10^4$ and $\binom{9600}{2} \times 3^2 = 4.1 \times 10^8$, respectively. Since the number of newly produced virions per day is higher than that of all possible mutations, all possible one-nucleotide and two-nucleotide mutants seem to be produced multiple times each day and preexist before treatment (25, 26) (**Fig. 4c** and **d**).

We estimated the anti-HCV effect of each drug combination at their clinical concentrations by applying a drug combination theory, Bliss independence (20, 22-24) (see **Supplementary Fig. S7** and **S10**). Bliss independence assumes that each drug acts on different targets, and is defined as follows for double-combinations:

$$f_u^{Bcom} = f_u^A \times f_u^B, \quad (S8)$$

where f_u^{Bcom}, f_u^A and f_u^B are the fractions of HCV replication events unaffected by the combined drugs A and B, single drug A and single drug B, respectively (see also **Supplementary Note 3** for triple-combinations). Using Eq. (S8), we determined the fractions of production events unaffected by the combined drugs A and B from that of the single drugs based on the estimated values of IC_{50} and *m*, and clinical concentrations of each drug (1, 27) (see **Table S4**). The fractions of unaffected production events of each double-drug and triple-drug combination are shown in **Supplementary Fig.**

S11a and **b**, respectively. Among the current clinically relevant double DAA-combinations (SOF&SMV, DCV&SOF, DCV&ASV, and LDV&SOF), SOF&SMV at clinical concentration showed lowest f_u^{Bcom}, which was followed by DCV&SOF, DCV&ASV, and LDV&SOF (**Supplementary Fig. S11a**) and the highest IIP^{Bcom} (**Fig. 4a**). Interestingly, the DCV&SMV combination, which is under clinical development (28), presents the highest IIP^{Bcom} and the lowest f_u^{Bcom} among the 15 possible combinations. This suggests that the combination of DCV&SMV is the most effective drug combination to suppress HCV production among the current choices of double-DAA combinations. Among triple DAA combinations, SOF&DCV&SMV showed further improvement in IIP^{Bcom}. This triple combination achieved the highest IIP^{Bcom} and the lowest f_u^{Bcom} among the 8 triple-combinations (**Fig. 4b** and **Supplementary Fig. S11**).

Based on the estimated antiviral activity of the clinically major multidrug combinations (i.e., 15 double-combinations and 6 triple-combinations) under the clinical concentrations, we calculated the expected number of newly produced virions carrying one-nucleotide or two-nucleotide mutations after one day of treatment in **Fig.4c** and **d** (i.e., $f_u^{Bcom} \times P_1 \times 10^{12}$ and $f_u^{Bcom} \times P_2 \times 10^{12}$, respectively). DCV&SMV presented the lowest chance for mutant viruses to emerge, stressing an advantage of this combination. The combination of SMV&SOF shows a relatively low number of emerging mutants within the 15 considered drug combinations, which is consistent with our cell culture analyses of IIP^{com} (**Fig. 3a** and **Supplementary Fig. S6**). This result explains the excellent clinical performance of SMV&SOF (>90% SVR) in both treatment naïve patients and non-responders to IFN-based therapy as well as in liver transplant recipients (29, 30).

Notice there is still a chance of producing all possible one-nucleotide mutants after the first day of therapy for the majority of the double-drug combination treatments (**Fig. 4c**). However, treatment with any of the double-DAA and triple-DAA combinations can decrease the newly produced mutants with two-nucleotide substitutions below the level covering all the patterns of possible two-nucleotide mutants (**Fig. 4c** and **d**). Thus, these combinations effectively reduce the probabilities that two-nucleotide mutants occur coincidently during treatment, and therefore, the probabilities to generate drug resistance.

Supplementary Note 5: Comparison of the anti-HCV quantification analysis between the replicon and the infectious systems

In this study, HCV replication was evaluated using an HCV replicon (genotype 1b) carrying a luciferase gene fused with a neomycin-resistant gene. Using this replicon enables one to produce in a high throughput manner the large quantity of data that are required for the quantification analysis of antiviral activity of drugs. We confirmed the validity of using this replicon system for the quantification analysis of drugs with the following two assays.

We examined whether the antiviral profiles of DAAs observed in the replicon system were essentially equivalent to those provided in a more physiologically relevant condition, an HCV infectious system (31-33). As genotype 1 HCV in the infectious system propagates with low efficiency and is not appropriate for the robust quantification analysis (34, 35), we used a genotype 2 strain, JFH-1, which propagate efficiently both in the replicon and the infectious system as a model (31, 36). SMV, ASV, DCV, LDV, DAS, and SOF as different classes of DAAs, were treated either mono-, double-, or triple-combinations to Huh-7 cells infected with HCV JFH-1 (31) or transfected with a JFH-1 replicon RNA (19) for 72 hours. HCV production and replication were evaluated by monitoring the infectivity of HCV in culture supernatant by focus formation assay and the activity of luciferase in the cells by luciferase assay, respectively. The reduction in relative HCV production/replication was examined for various concentrations of DAAs (0.25, 0.5, 1, 2, and 4 x IC_{50}) with single, double, and triple treatments. Based on the results for 6 single, 15 double, and 6 triple combinations (**Supplementary Fig. S12**), we calculated IIPs. We note, Spearman's rank-order correlation analysis found statistically significant correlations of IIPs obtained in the replicon system with those obtained in the infectious culture systems for both single ($\rho = 0.886$), double ($\rho = 0.725$), and triple ($\rho = 0.886$) combinations (**Supplementary Fig. S12**). These results clearly suggest that the anti-HCV activity of drugs based on the intrinsic antiviral activity obtained in the replicon assay is correlated with that in the HCV infectious culture system. Second, we examined whether introduced adaptive mutations in the replicon significantly affect our quantification analysis of drugs, To test this point, we compared the antiviral profiles of single DAA treatment in a cell culture-adapted replicon (genotype 1b) with those in a non-cell culture adapted Con1 (genotype 1b) replicon in Huh-7 cells overexpressing SEC14L2 (37) in a similar manner to the experiments shown above. This assay also revealed significant correlations of IIPs between the replicons with and without adaptive mutations **(Supplementary Fig. S13**) ($\rho = 0.60$). These results suggest that the IIPs measured in our genotype 1 replicon reflect the anti-HCV property of drugs, irrespective of the existence of adaptive mutations. Thus, our method is useful for quantifying the anti-HCV activity of drugs.

References

1. Friborg J*, et al.* (2014) In Vitro Assessment of Re-treatment Options for Patients with Hepatitis C Virus Genotype 1b Infection Resistant to Daclatasvir Plus Asunaprevir. *Infect Dis Ther*.
2. Reddy MB*, et al.* (2012) Pharmacokinetic/Pharmacodynamic predictors of clinical potency for hepatitis C virus nonnucleoside polymerase and protease inhibitors. *Antimicrob Agents Chemother* 56(6):3144-3156.
3. Jilek BL*, et al.* (2012) A quantitative basis for antiretroviral therapy for HIV-1 infection. *Nature medicine* 18(3):446-451.
4. Laskey SB & Siliciano RF (2014) A mechanistic theory to explain the efficacy of antiretroviral therapy. *Nat Rev Microbiol* 12(11):772-780.
5. Sampah ME, Shen L, Jilek BL, & Siliciano RF (2011) Dose-response curve slope is a missing dimension in the analysis of HIV-1 drug resistance. *Proc Natl Acad Sci U S A* 108(18):7613-7618.
6. Shen L*, et al.* (2008) Dose-response curve slope sets class-specific limits on inhibitory potential of anti-HIV drugs. *Nature medicine* 14(7):762-766.
7. Shen L*, et al.* (2011) A critical subset model provides a conceptual basis for the high antiviral activity of major HIV drugs. *Sci Transl Med* 3(91):91ra63.
8. Shen L, Rabi SA, & Siliciano RF (2009) A novel method for determining the inhibitory potential of anti-HIV drugs. *Trends Pharmacol Sci* 30(12):610-616.
9. Vrolijk JM*, et al.* (2003) A replicon-based bioassay for the measurement of interferons in patients with chronic hepatitis C. *J Virol Methods* 110(2):201-209.
10. Cha A & Budovich A (2014) Sofosbuvir: a new oral once-daily agent for the treatment of hepatitis C virus infection. *P t* 39(5):345-352.
11. Pawlotsky JM (2014) New hepatitis C therapies: the toolbox, strategies, and challenges. *Gastroenterology* 146(5):1176-1192.
12. Liang TJ & Ghany MG (2013) Current and future therapies for hepatitis C virus infection. *N Engl J Med* 368(20):1907-1917.
13. Halfon P & Locarnini S (2011) Hepatitis C virus resistance to protease inhibitors. *J Hepatol* 55(1):192-206.
14. Wong KA, Xu S, Martin R, Miller MD, & Mo H (2012) Tegobuvir (GS-9190) potency against HCV chimeric replicons derived from consensus NS5B sequences from genotypes 2b, 3a, 4a, 5a, and 6a. *Virology* 429(1):57-62.
15. Svarovskaia ES*, et al.* (2014) Infrequent development of resistance in genotype 1-6 hepatitis C virus-infected subjects treated with sofosbuvir in phase 2 and 3 clinical trials. *Clinical infectious diseases : an official publication of the Infectious Diseases Society of America* 59(12):1666-1674.
16. Horner SM & Gale M, Jr. (2013) Regulation of hepatic innate immunity by hepatitis C virus. *Nature medicine* 19(7):879-888.
17. Gaither LA*, et al.* (2010) Multiple cyclophilins involved in different cellular pathways mediate HCV replication. *Virology* 397(1):43-55.
18. Tanabe Y*, et al.* (2004) Synergistic inhibition of intracellular hepatitis C virus replication by combination of ribavirin and interferon- alpha. *J Infect Dis* 189(7):1129-1139.
19. Kato T*, et al.* (2005) Detection of anti-hepatitis C virus effects of interferon and ribavirin by a sensitive replicon system. *J Clin Microbiol* 43(11):5679-5684.
20. Greco WR, Bravo G, & Parsons JC (1995) The search for synergy: a critical review from a response surface perspective. *Pharmacol Rev* 47(2):331-385.
21. Tallarida RJ (2001) Drug synergism: its detection and applications. *J Pharmacol Exp Ther* 298(3):865-872.
22. Koizumi Y & Iwami S (2014) Mathematical modeling of multi-drugs therapy: a challenge for determining the optimal combinations of antiviral drugs. *Theor Biol Med Model* 11:41.

23. Bliss C (1939) The toxicity of poisons applied jointly1. *Annals of applied biology* 26(3):585-615.
24. Kobayashi T*, et al.* (2014) Quantification of deaminase activity-dependent and -independent restriction of HIV-1 replication mediated by APOBEC3F and APOBEC3G through experimental-mathematical investigation. *J Virol* 88(10):5881-5887.
25. Rong L, Dahari H, Ribeiro RM, & Perelson AS (2010) Rapid emergence of protease inhibitor resistance in hepatitis C virus. *Sci Transl Med* 2(30):30ra32.
26. Neumann AU*, et al.* (1998) Hepatitis C viral dynamics in vivo and the antiviral efficacy of interferon-alpha therapy. *Science* 282(5386):103-107.
27. Lalezari J*, et al.* (2015) Ombitasvir/paritaprevir/r and dasabuvir plus ribavirin in HCV genotype 1-infected patients on methadone or buprenorphine. *J Hepatol* 63(2):364-369.
28. Zeuzem S*, et al.* (2016) Daclatasvir plus simeprevir with or without ribavirin for the treatment of chronic hepatitis C virus genotype 1 infection. *J Hepatol* 64(2):292-300.
29. Lawitz E*, et al.* (2014) Simeprevir plus sofosbuvir, with or without ribavirin, to treat chronic infection with hepatitis C virus genotype 1 in non-responders to pegylated interferon and ribavirin and treatment-naive patients: the COSMOS randomised study. *Lancet* 384(9956):1756-1765.
30. Brown RS, Jr.*, et al.* (2016) Interferon-free therapy for genotype 1 hepatitis C in liver transplant recipients: Real-world experience from the hepatitis C therapeutic registry and research network. *Liver Transpl* 22(1):24-33.
31. Wakita T*, et al.* (2005) Production of infectious hepatitis C virus in tissue culture from a cloned viral genome. *Nature medicine* 11(7):791-796.
32. Zhong J*, et al.* (2005) Robust hepatitis C virus infection in vitro. *Proc Natl Acad Sci U S A* 102(26):9294-9299.
33. Lindenbach BD*, et al.* (2005) Complete replication of hepatitis C virus in cell culture. *Science* 309(5734):623-626.
34. Yi M, Villanueva RA, Thomas DL, Wakita T, & Lemon SM (2006) Production of infectious genotype 1a hepatitis C virus (Hutchinson strain) in cultured human hepatoma cells. *Proc Natl Acad Sci U S A* 103(7):2310-2315.
35. Kato T*, et al.* (2007) Production of infectious hepatitis C virus of various genotypes in cell cultures. *J Virol* 81(9):4405-4411.
36. Kato T*, et al.* (2003) Efficient replication of the genotype 2a hepatitis C virus subgenomic replicon. *Gastroenterology* 125(6):1808-1817.
37. Saeed M*, et al.* (2015) SEC14L2 enables pan-genotype HCV replication in cell culture. *Nature* 524(7566):471-475.